J Appl Biomed
DOI: 10.32725/jab.2025.018
journal homepage: http://jab.zsf.jcu.cz

Journal of Applied Biomedicine

Original research article

Exosomes from LPS-stimulated macrophages alleviate neuroinflammatory responses by reducing pyroptosis in systemic lipopolysaccharide-induced mice

Tao Ying, Zhezhe Sun *

The First Affiliated Hospital of Ningbo University, Department of Neurology, Ningbo 315000, China

Abstract
Central nervous system (CNS) inflammation occurs in cognitive dysfunction, but the underlying mechanisms remain unclear. The newly discovered pattern of cell death in recent years is called pyroptosis, which is distinguished from apoptosis and necrosis, and is mainly dependent on caspase-1 mediated inflammatory response. Stem-derived exosomes have immunomodulatory and immunosuppressive effects. In the present study, we aimed to investigate the exosomes (Ex) secreted by lipopolysaccharide (LPS)-stimulated macrophages (LPS-Ex) to attenuate the neuroinflammatory response caused by systemic LPS stimulation by attenuating pyroptosis. We studied lipopolysaccharide (LPS)-induced cognitive impairment and neuroinflammation in C57BL/6 mice by behavioral testing, immunofluorescence, enzyme-linked immunosorbent assay (ELISA), Western blotting, and other methods. We found that LPS-Ex can reduce the level of inflammatory factors, down-regulate the pyroptosis pathway and the inflammatory pathway of NF-κB, and improve the inflammatory response of neurological function in mice. The conclusion is that LPS-Ex relieves neuroinflammation by reducing pyroptosis. It can be used as a novel therapeutic strategy for neuroprotection and functional recovery in the onset of central nervous system inflammation.

Keywords: Exosomes; Lipopolysaccharide; Neuroinflammation; Pyroptosis

Highlights:
- LPS-Ex alleviates neuroinflammation by reducing pyroptosis.
- LPS-Ex alleviates neuroinflammation by inhibiting the NF-κB pathway.
- LPS-Ex can be used as a new therapeutic strategy for neuroprotection and functional recovery in the early stage of central nervous system inflammation.

Introduction

Recently, brain inflammation has been shown to play an important role in the development and progression of brain dysfunction, such as cognitive deficits and depression and anxiety (Vezzani and Granata, 2005). It is considered to be the main cause of high morbidity and mortality in clinical patients. In particular, cognitive decline caused by inflammation of the central nervous system (CNS) is receiving increasing attention (Lee et al., 2019). However, the molecular mechanisms involved in CNS inflammation remain unknown.

Microglia are macrophages that reside in the brain and respond quickly to nervous system inflammatory activation (Hu et al., 2015). Pyroptosis is a highly specific inflammatory programmed cell death that differs from necrosis or apoptosis (Shi et al., 2017). It relies on extracellular detection of acute injury to identify extracellular and intracellular pathogen-associated molecular patterns (PAMP) by Pattern Recognition Receptors (PRRs). PRRs can trigger the formation of multiprotein complexes, called inflammatory bodies (inflammasomes), which also contain apoptosis-associated spot-like proteins (ASCs) and pre-caspase-1, which process signals to induce a series of inflammatory responses (Man et al., 2017). Pyroptosis can occur in neurons, astrocytes, and microglia in damaged brain tissue, where it accelerates the induction of inflammation and neuronal death and aggravates neurological outcomes (Lee et al., 2018). Therefore, alleviating the pyroptosis response in the brain may be a way to alleviate neuroinflammation.

Exosomes are small membrane particles of 40–150 nm size that play a key role in cell-cell communication by delivering miRNA to recipient cells (Denzer et al., 2000). Related studies have shown that exosomes secreted by macrophages contain elevated levels of cytokines and miRNAs and regulate inflammation by converting early pro-inflammatory gene transcription into anti-inflammatory gene transcription.

* **Corresponding author:** Zhezhe Sun, The First Affiliated Hospital of Ningbo University, Department of Neurology, Ningbo 315000, China; e-mail: sunzhezhe101010@163.com
http://doi.org/10.32725/jab.2025.018
Submitted: 2025-06-30 • Accepted: 2025-12-05 • Prepublished online: 2025-12-08
J Appl Biomed 23/4: 163–173 • EISSN 1214-0287 • ISSN 1214-021X

Compared to macrophage-derived exosomes, exosomes secreted by LPS-stimulated macrophages carry higher levels of three miRNAs, which inhibit the transcription and translation of pro-inflammatory cytokines, thereby helping to eliminate inflammation in recipient cells. In LPS stimulated macrophages, three anti-inflammatory-related miRNAs (miR-126-5p, miR-21# or miR-21-3p and miR-212) were up-regulated in exosomes, indicating the potential role of LPS-Ex in inhibiting inflammation (Hsu et al., 2011; Zheng et al., 2019). All in all, LPS-stimulated macrophage-derived exosomes have shown significant anti-inflammatory effects on stroke (Zheng et al., 2019). Therefore, we examined the possibility of using exosomes secreted by lipopolysaccharide (LPS)-stimulated macrophages (LPS-Ex) as a treatment.

We hypothesized that LPS-Ex can promote anti-inflammatory responses by reducing pyroptosis, thereby reducing neuroinflammatory damage and modulating the brain microenvironment to achieve neuroprotection.

Materials and methods

Animals and grouping

In this study, adult male C57BL/6 mice (8–10 weeks old, 20–25 g) were purchased from Shanghai Slaccas Experimental Animal Limited Liability Company (Shanghai, China). All procedural and ethical considerations were approved by the Experimental Animal Ethics Committee of Ningbo University. The mice were kept for one week and then randomly divided into three groups (a total of 150 mice, with 50 mice in each group): Control group, LPS injection group, LPS-Ex injection group. Lipopolysaccharide (*Escherichia coli* O111: B4, Sigma-Aldrich, USA) was diluted in saline and injected (1 mg/kg, intraperitoneally) into the LPS injection group and LPS-Ex injection group. Physiological saline was administered to the control group. Mouse modeling refers to mice that have been injected with LPS.

Exosomes' preparation, purification, and administration

Mouse macrophage RAW264.7 cell line was purchased from the American Type Culture Collection (ATCC) and in Dulbecco's Modified Eagle Medium (DMEM, Hyclone, UT, USA), containing 10% fetal bovine serum (FBS; Gibco, CA, USA) and 1% penicillin-streptomycin (PS). The cells were maintained in a humidified cell incubator at 37 °C, 5% carbon dioxide (CO_2). Preparation and purification of Ex and LPS-Ex were as described previously (Zheng et al., 2019). To obtain LPS-Ex, 100 ng/ml LPS was added to the cell culture dish to stimulate RAW 264.7 cells. After continuous incubation for 24 h, the supernatant was centrifuged at 2 000 × g for 10 min, then 10 000 × g, centrifuged at 4 °C for 30 min to remove cells and debris, and then filtered using a 0.22 μm filter (Millipore, Billerica, MA, USA), the filtrate was centrifuged at 120 000 × g for 120 min at 4 °C in a Type CS150GXII ultracentrifuge (Hitachi, Koki, Co., Ltd, Japan). This step yields exosome pellet. The exosome pellet was resuspended in phosphate buffered saline (PBS) and again centrifuged at 120 000 × g for 150 min. Subsequently, the pelleted exosomes were suspended in PBS and analyzed using a BCA protein assay kit (Beyotime, Shanghai, China). The morphology and shape of LPS-Ex were measured by a transmission electron microscope (JEM-1200EX; JEOL, Tokyo, Japan). The characteristics of the isolated exosomes were evaluated by Western blot through the detection of CD63 (Mouse, Santa Cruz, sc-5275, 1:500), TSG101 (Rabbit, Abcam, ab125011, 1:1000), and cytochrome c (Rabbit, CST, 11940s, 1:1000) expression. The particle size distribution was analyzed by Zetasizer (Malvern, ZETASIZER Nano series-Nano-ZS) according to the manufacturer's instructions. 1 mg of LPS-Ex was suspended in 0.5 ml of PBS and administered to the tail vein by a single intravenous injection. In addition, 0.5 ml of PBS was administered intravenously as a control for the LPS group. LPS-Ex was injected 60 min after mouse modeling. Here, the mouse modeling refers to the injection of LPS into mice.

Hematoxylin-Eosin (H&E) staining

Animals were anesthetized, then perfused through the heart with cold 0.9% saline and then perfused with 4% paraformaldehyde (PFA) in PBS for fixation. Brains were harvested and fixed in 4% PFA for 24 h and then dehydrated with 30% sucrose for 48 h. The dehydrated brain was embedded with an optimal cutting temperature compound (OCT) for cutting. Serial coronal sections (10 mm thick) were cut using a cryostat (Leica Biosystems, CM1950) and stored at 20 °C. The portion of the lesion center has the lowest spare tissue and the largest lesion area. H&E staining was performed at the injury center using an H&E staining kit (Solarbio, China) according to the manufacturer's instructions. Quantitation was done by ImageJ (National Institutes of Health, Bethesda).

Western blot

The post-brain protein was extracted with phenylmethylsulfonyl fluoride (PMSF; Beyotime) in pre-cooled radioimmunoprecipitation assay buffer (RIPA). The protein concentration was measured using a PierceTM BCA Protein Assay Kit (Thermo Scientific). 50 μg of total protein were separated using 12% (SDS-PAGE) and then transferred to a PVDF membrane (Millipore Corp). The membrane was blocked with 5% milk for 2–3 h at room temperature and then incubated overnight with the following specific primary antibody: NLRP3 (1:1000, Abcam), GSDMD (1:1000, Abcam), NF-κB (1:1000; Cell Signaling Technology [CST], Danvers, MA, USA), p-NF-κB (1:1000; Cell Signaling Technology [CST], Danvers, MA, USA), p-IκBα (1:1000, CST), IκBα (1:1000, CST), ASC (1:1000; Santa Cruz Biotechnology, Dallas, TX, USA), cleaved-caspase-1 (1:1000, CST), Caspase-11 (1:1000, Abcam), TLR4 (1:1000, Proteintech), Glyceraldehyde 3-phosphate dehydrogenase (GAPDH; 1:1000, CST) and β-actin (1:1000; Abcam). After washing with TBST, the membrane was incubated with the secondary antibody for 1 h. Finally, the protein bands were observed with ECL reagent.

Neurobehavioral tests

mNSS (modified Neurological Severity Score) including sensory, motor, reflex and balance tests were used to assess neurobehavioral behavior (Ni et al., 2019). The neurological function score was 0–18 (normal score, 0; maximum defect score, 18). Mice were trained and evaluated prior to surgery to ensure a normal score of zero. Then, the neurobehavioral defect scores were recorded by blind test at 12 h, 24 h, 48 h, and 72 h after modeling.

The rotarod test was carried out as described previously (Ni et al., 2019). Rotating rod testing assesses fine motor coordination and balance by measuring the ability of mice to remain on a rotating rod (RWD Life Science, San Diego, CA, USA). One day before modeling, the mice were first subjected to an adaptability test (rotation speed: 4 rpm), and then another four tests were performed to accelerate the rotation speed (from 4 to 40 rpm in 5 min). The average time the rod was dropped

during the test was recorded to obtain a stable pre-injury baseline value. Each mouse was tested four times a day at the same rate at 12, 24, 48, and 72 h after modeling, with an interval of 30 min, and the mean descending latency was measured.

Assessment of cerebral edema

Brain water content (BWC) is a sensitive method for measuring cerebral edema, quantified using dry and wet methods, as detailed in previous studies (Ishrat et al., 2015). Mice were sacrificed under deep anesthesia at various time points after injury, and brain tissue was quickly removed. Tissue samples were then weighed to determine wet weight (WW). The sample was dried in an oven at 100 °C for 24 h to obtain a dry weight (DW). BWC is calculated by the following formula: 100%× (WW-DW)/WW.

Lactate dehydrogenase release detection

Blood was collected from mice through the tail vein after deep anesthesia (centrifugation at 3 000 × g for 10 min) and serum lactate dehydrogenase (LDH) release was measured using a commercial kit (Solarbio, Beijing, China). After transferring 100 μl of serum or supernatant to a 96-well plate, we added the reaction mixture and incubated for 30 min at room temperature in the dark. The LDH concentration was quantified by measuring the absorbance at 490 nm (Sun et al., 2020).

Caspase-1 activity assay

Caspase-1 activity was measured using a colorimetric assay (Beyotime, Haimen, China) according to the manufacturer's protocol. Brain tissue was homogenized in ice-cold RIPA buffer containing 1 mM phenylmethylsulfonyl fluoride (PMSF) and centrifuged at 20 000 × g for 10 min at 4 °C. The supernatant was collected and incubated with acetyl-Tyr-Val-Ala-Asp p-nitroanilide (Ac-YVAD-pNA) (2 mM) for 2 h at 37 °C. The pNA was quantified at 405 nm on a Molecular Devices M2 plate reader (Molecular Devices Corporation, San Jose, CA, USA). Caspase-1 activity was determined by serial dilution of a standard curve derived from the pNA standard and normalization to total protein. The protein concentration was measured using the Bradford method to ensure a concentration of 1–3 μg/μl. Data are expressed as relative caspase-1 activity opposite to the control (Sun et al., 2020).

Terminal deoxynucleotidyl transferase-mediated dUTP-biotin nick end labeling (TUNEL) staining

Apoptosis was measured by TUNEL staining using the TUNEL Apoptosis Assay Kit (Beyotime). TUNEL stained apoptotic nuclei, 4', 6-diamidino-2-phenylindole (DAPI) with fluorescein-in-dUTP stained all nuclei. The apoptotic index (AI) was calculated as the number of TUNEL positive cells divided by the total number of cells per cell. AI was evaluated in 15 randomly selected fields.

Histomorphological examination

The tissue staining sections were finally observed under an optical microscope (RWD, Shenzhen, China) and a fluorescence microscope (Olympus IX81, Tokyo, Japan).

Immunohistochemical analysis

According to the approved animal protocol, mice were euthanized by inhaling 8% isoflurane and their brain tissues were removed. Immediately after removal of the brain, brain tissue was incubated in 4% paraformaldehyde in phosphate buffered saline (PBS) and embedded in paraffin for sectioning. After paraffin sections were rehydrated and washed twice in PBS, endogenous peroxidase activity was blocked with 3% H_2O_2 for 10 min. The antigen was cross-linked in an autoclave for 3 min and then the sample was washed twice in PBS. All formulations were then treated with goat serum blocking reagent (Abcam, ab7481) for 45 min. Excess reagent was removed by rapid rinsing with PBS. The sections were incubated with the primary antibody (Caspase-1, 1:500, Abcam) overnight. After washing twice in PBS, a secondary antibody (ASS3403; Abgent, San Diego, CA, USA) was added to all slides for 30 min. Excess reagent was removed and the slides were washed in PBS and incubated with DAB (Solarbio, DA1010) for 5–10 min until the desired color appeared. All preparations were counterstained with hematoxylin (Solarbio, G1120) for 30 s. Protein expression was determined in four adjacent sections for each sample.

Immunofluorescence staining

The brain was collected and immediately immersed in an aldehyde fixative (10% formaldehyde in 0.1% sodium phosphate buffer) in 4% paraformaldehyde and kept at 4 °C for 2 days. Next, the brain tissue was fixed in 30% sucrose until it sank to the bottom of the container. Brain tissue was then removed for embedding in an optimal cutting temperature (OCT) composite frozen section. Brain frozen sections were fixed with acetone at –20 °C for 20 min and incubated in 3% bovine serum albumin solution (BSA, Sigma-Aldrich) for 30 min at 37 °C to block non-specific staining. Sections were then incubated overnight at 4 °C with the following antibodies: ionized calcium binding adaptor 1 (Iba-1, 1:500, Abcam), NeuN (1:500, Abcam). Thereafter, the frozen sections were washed with PBS and incubated with the corresponding secondary antibody (Alexa Fluor 594: donkey anti-goat; Alexa Fluor 488: donkey anti-rabbit; Invitrogen) for 1 h at room temperature. Finally, the nuclei were counterstained with DAPI (Abcam). Images of each section were captured using a fluorescence microscope (Olympus IX81, Tokyo, Japan). The images of each part were collected under a fluorescence microscope, and the data were analyzed by randomly selecting 15 fields of view (5 fields of view per section × 3 sections per mouse) under the microscope through ImageJ software (National Institutes of Health, Bethesda).

Enzyme-linked immunosorbent assay

The levels of transforming-growth factor TGF-β, TNF-α, IL-10, IL-1β, NF-κB, and IL-18 were measured using an enzyme-linked immunosorbent assay (ELISA) kit (Boyun, Shanghai, China) according to the manufacturer's instructions.

Statistical analysis

Data are expressed as mean ± standard deviation. All values were analyzed using Prism software (GraphPad, USA). To compare differences involving three or more groups, one-way or two-way analysis of variance (ANOVA) was used. A *p*-value of less than 0.05 or 0.01 or 0.001 is considered to be statistically significant.

Results

Characterization of LPS-Ex and changes in inflammation in mice serum and brain over time

First, to better understand the characteristics of exosomes, exosomes were evaluated by TEM and Western blotting. TEM shows the presence of exosomes, small membrane vesicles of 30 to 150 nm in size (Fig. 1A). The average size of the LPS-Ex is 117.3 nm. Macrophages produce particles with a peak dia-

meter of 138.1 nm after LPS stimulation (Fig. 1B). LPS-Ex was found to express high levels of TSG101 and CD63 (Fig. 1C). TSG101 and CD63 are commonly used indicators for detecting the success of exosome extraction (Ni et al., 2019). Next, we examined changes in inflammatory factors in serum and brain over time in mice injected intraperitoneally with LPS. We measured the levels of IL-1β, NF-κB, and IL-18 in serum and brain at 12 h, 24 h, 48 h, and 72 h after LPS injection by ELISA, and found that the inflammatory factors were highest at 24 h (Fig. 1D–I). After that, we examined the changes in brain water content at 12 h, 24 h, 48 h, and 72 h after LPS injection, and found that the degree of cerebral edema was highest at 24 h (Fig. 1J).

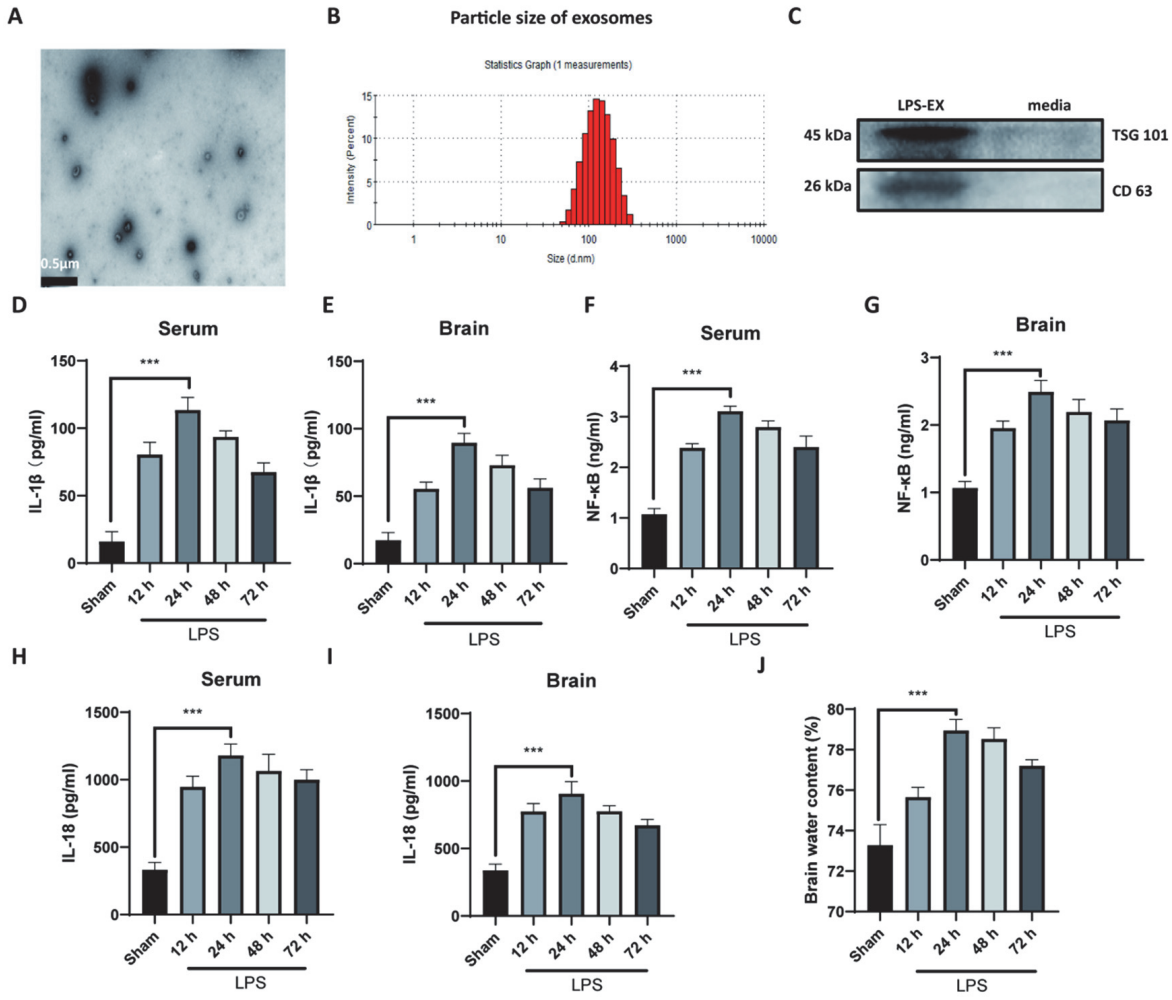

Fig. 1. The characteristics of LPS-Ex and the changes of inflammation in mouse serum and brain at different time points. (**A**) The morphology of exosomes in TEM. (**B**) The X-axis represents the size distribution of exosomes. The average size of LPS-Ex is 117.3 nanometers. The peak diameter of the particles produced by macrophages after LPS stimulation was 138.1 nanometers. (**C**) Through protein immunoimprinting, LPS-Ex was found to express high levels of TSG101 and CD63. (**D–I**) We used ELISA to detect the changes in the concentrations of IL-1β, NF-κB, and IL-18 in serum and brain tissue at different time points. This was an experiment directly between the sham group and the LPS group. (**J**) The changes of brain water content at different time points; $n = 6$ per group. *** $P < 0.001$. Data are presented as the mean ± SD.

LPS-Ex can alleviate serum and brain inflammatory factors levels 24 h after LPS injection

We measured the expression levels of inflammatory factors (TNF-α, NF-κB, IL-1β, IL-18, IL-10, and TGF-β) by ELISA in serum and brain, and found that LPS-Ex treatment relieved after 24 h. The levels of inflammatory factors (TNF-α, NF-κB, IL-1β, IL-18) decreased significantly, and the levels of anti-inflammatory factors IL-10 and TGF-β increased, compared with the LPS injection alone (Fig. 2A–F).

In addition, we tested the activity of caspase-1 in the brain and found that LPS-Ex treatment resulted in lower caspase-1 activity than the LPS group (Fig. 2G). Previous studies have shown that pyroptosis is usually associated with released cytoplasmic LDH (DiPeso et al., 2017), we used the LDH test kit to detect the serum LDH content, and the treatment group showed less LDH (Fig. 2H). Therefore, LPS-Ex can alleviate the expression of pyroptosis-associated inflammatory factors.

LPS-Ex inhibits the pyroptosis pathway and NF-κB pathway and improves neurological prognosis

To investigate whether LPS-Ex can affect the expression of pyroptosis and inflammatory pathways, we checked the therapeutic effect of LPS-Ex by Western blotting at 24 h after LPS injection. We confirmed that LPS-Ex inhibits the expression of cleaved-caspase-1, NLRP3, ASC, and Gasdermin D

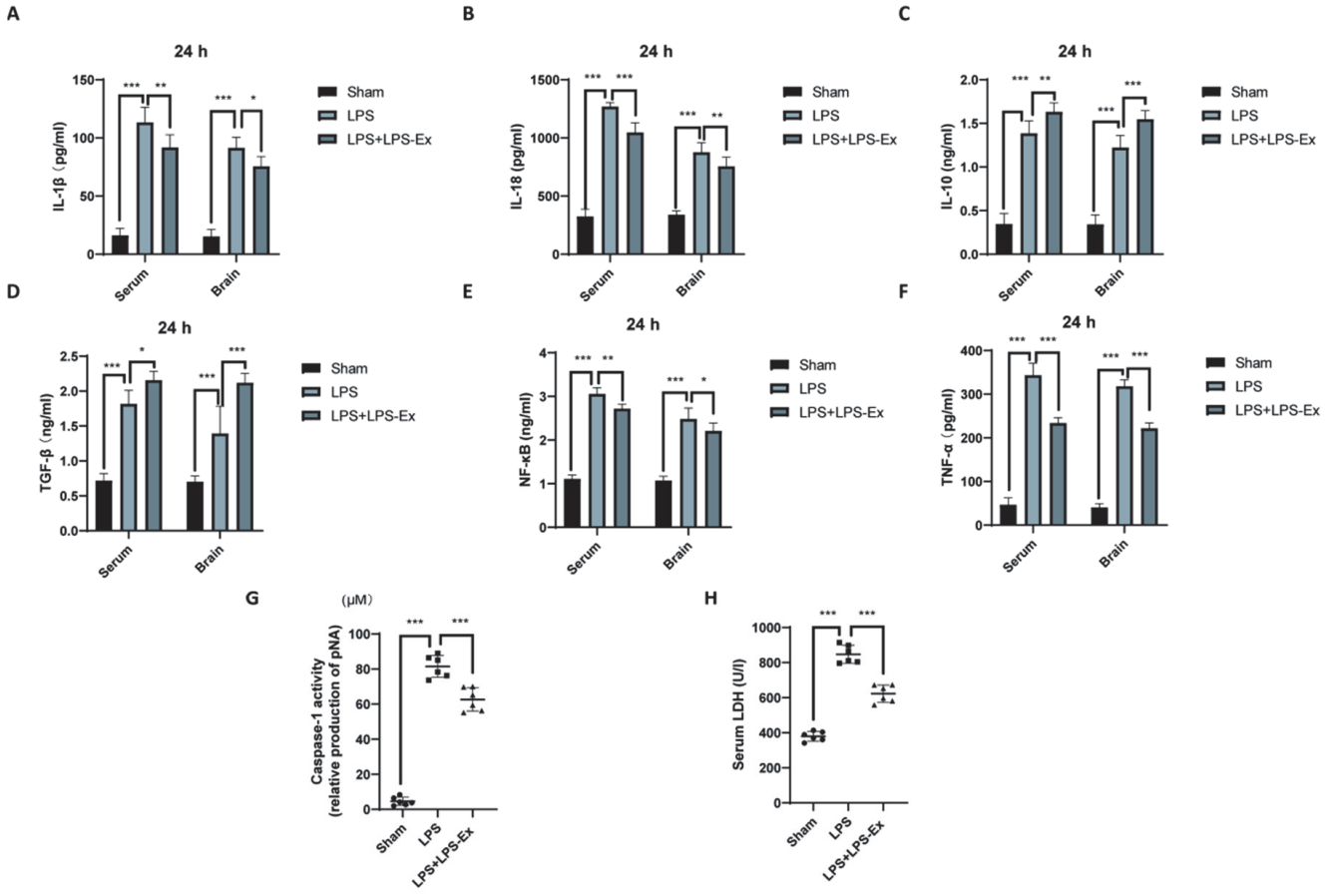

Fig. 2. The changes of inflammatory factor levels in serum and brain 24 h after LPS injection. (**A–F**) The changes of IL-1β, IL-18, IL-10, TGF-β, NF-κB, and TNF-α in serum and brain detected by ELISA. (**G**) Caspase-1 activity in brain tissue. (**H**) Lactate dehydrogenase (LDH) content in the serum; $n = 6$ per group. * $P < 0.05$, ** $P < 0.01$, *** $P < 0.001$. Data are presented as the mean ± SD.

(GSDMD) (Fig. 3A–F). GSDMD cleavage and pore formation are important components of pyroptosis in human cells (He et al., 2015). Caspase-11 is involved in the non-canonical pathway of pyroptosis (Kayagaki et al., 2015).

In addition, we quantified changes in the expression of NF-κB signaling factors in the brain 24 h after LPS injection. Toll-like receptors (TLRs) are important mediators of innate immunity. Unlike other TLR family members, TLR4 is specifically expressed in bone marrow-derived cells (such as mononuclear macrophages), and multiple studies have confirmed that TLR4 is closely related to neuroinflammation. NF-κB is located downstream of TLR4 and is in the cytoplasm when not activated. Upon activation, it induces phosphorylation of IκBα, thereby releasing NF-κB into the nucleus where it regulates the release of downstream inflammatory mediators through an inflammatory response (Courtois and Gilmore, 2006). We found that LPS-Ex inhibits the phosphorylation of both NF-κB and IκBα. At the same time, the TLR4 of the exosomes group was also reduced compared with the LPS group alone (Fig. 3G–J).

Regarding histological morphology, we did HE staining after 24 h. In the sham group, most of the neurons in the hippocampus showed clear cell structures with round and pale nuclei. After LPS injection, the atrophy of cell bodies and narrowing of the nucleus could be seen, especially in the Cornu Ammonis 1 (CA1) region. LPS-Ex led to a significant improvement in histomorphology (Fig. 4A–B).

In terms of neurological deficits, we found that the neurological function of the exosome treatment group improved at 24 h after LPS injection according to the mNSS score, the rotarod test, and the Y maze test (Fig. 4C–E). At the same time, we found that the degree of cerebral edema also improved (Fig. 4F).

LPS-Ex reduces microglia activation and neuronal apoptosis

We examined microglia in the cortex and hippocampus and found that the number of cells in different regions were decreased after LPS-Ex treatment observed by fluorescence microscope (Fig. 5A–D). We also found that the distribution of pyroptosis, according to the key protein caspase-1, was also reduced in the brain (Fig. 5E–H). In terms of apoptosis, we detected a decrease in neuronal apoptosis in different regions of the brain stained with TUNEL (Fig. 5I–N).

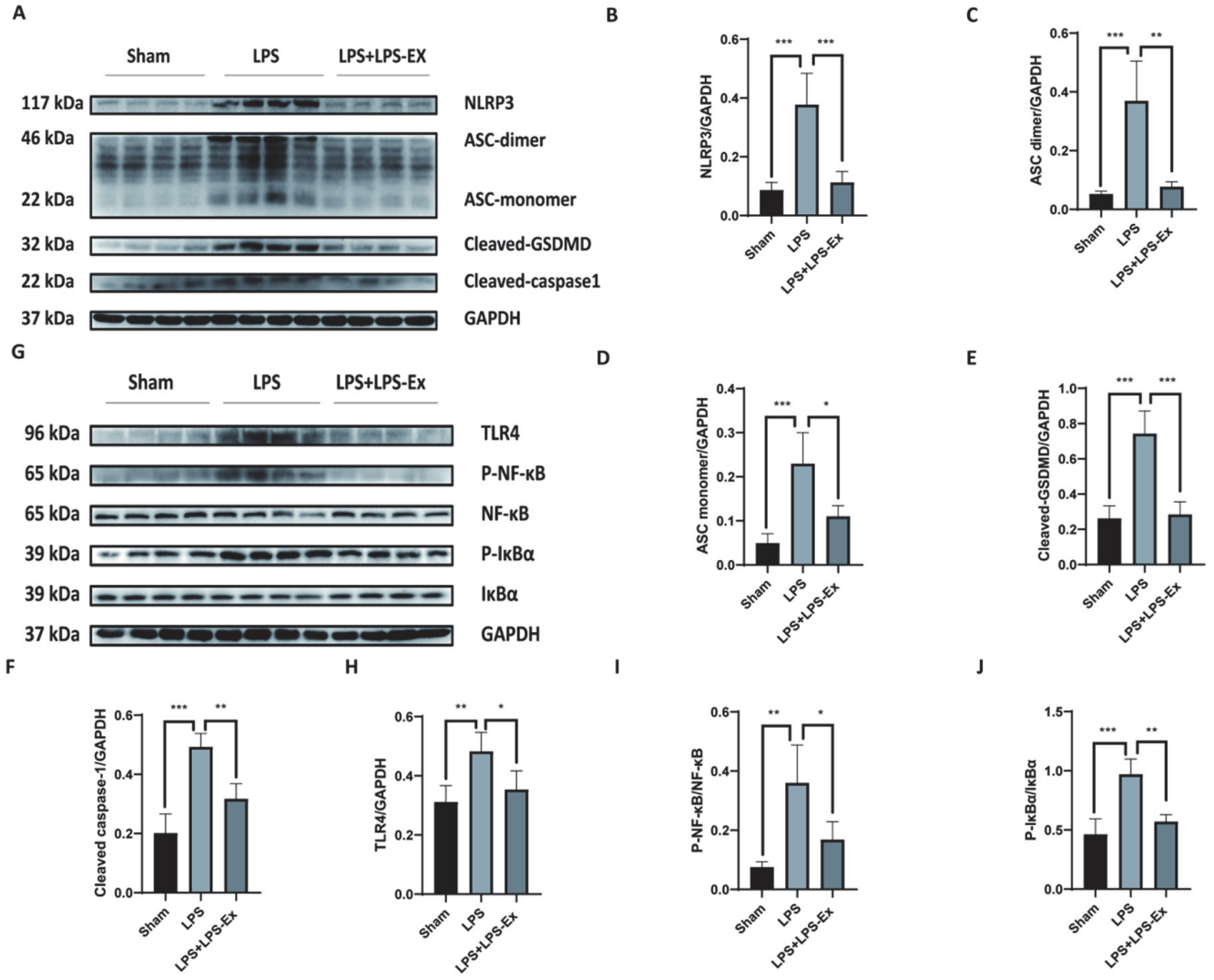

Fig. 3. LPS-Ex inhibits pyroptosis and NF-κB pathways. (**A–F**) The expressions of caspase-1, NLRP3, ASC, and GSDMD detected by Western blotting 24 h after LPS injection. (**G–J**) The expression of NF-κB signaling factors detected by Western blotting 24 h after LPS injection; $n = 4$ per group. * $P < 0.05$, ** $P < 0.01$, *** $P < 0.001$. Data are presented as the mean ± SD.

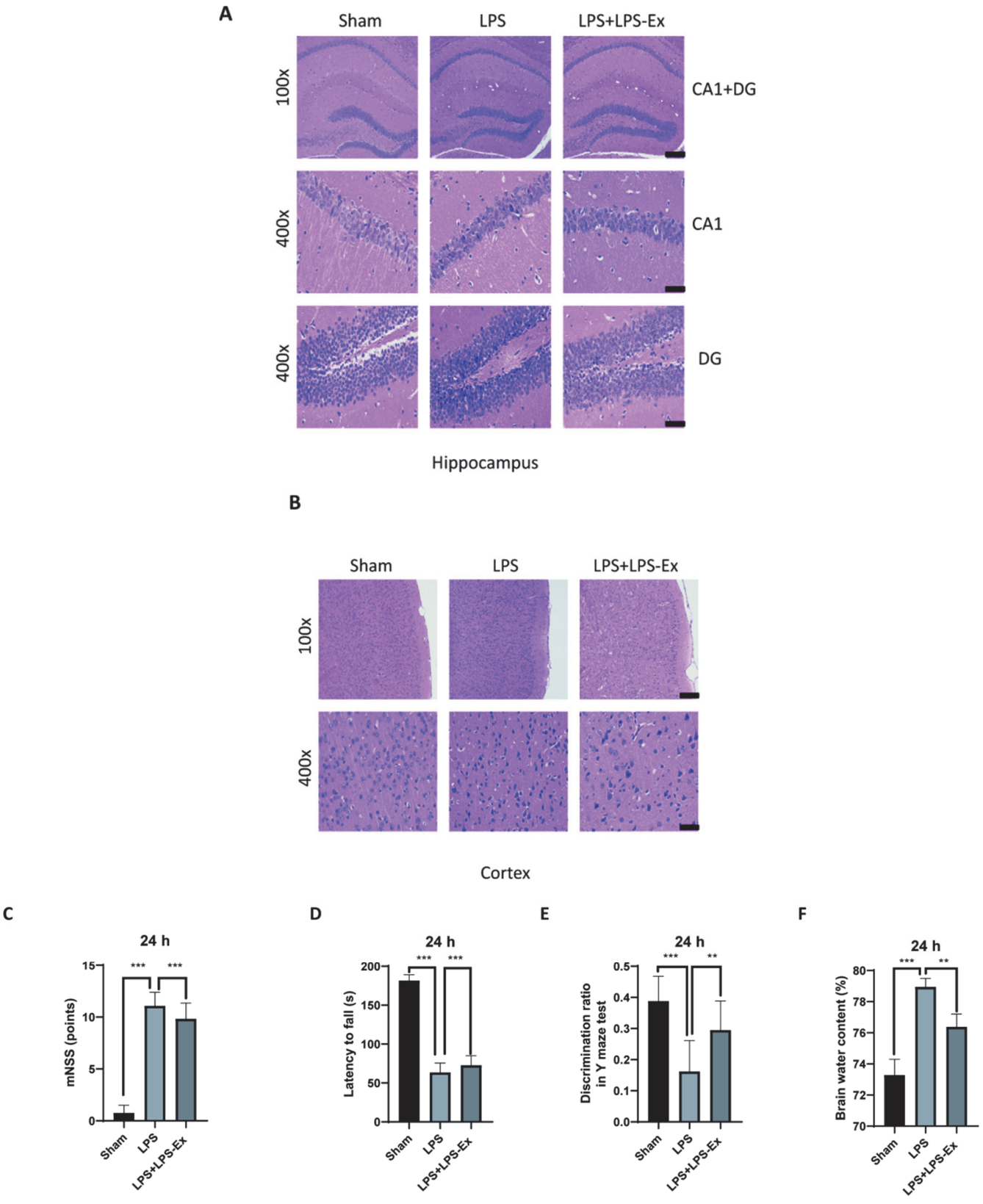

Fig. 4. LPS-Ex improves neurological prognosis. (**A–B**) Hematoxylin and eosin staining 24 h after LPS injection to detect the histomorphological changes of neurons in the hippocampus and cortex. The hippocampus includes Cornu Ammonis 1 (CA1) and Dentate Gyrus (DG). (**C–F**) Neurological deficits and cerebral edema of mice 24 h after LPS injection. The assessment of neurological deficits includes (**C**) the mNSS score, (**D**) the rotarod test, and (**E**) the Y maze test; $n = 6$ per group. * $P < 0.05$, ** $P < 0.01$, *** $P < 0.001$; 400x, Scale bar = 50 μm; 100x, Scale bar = 200 μm. Data are presented as the mean ± SD.

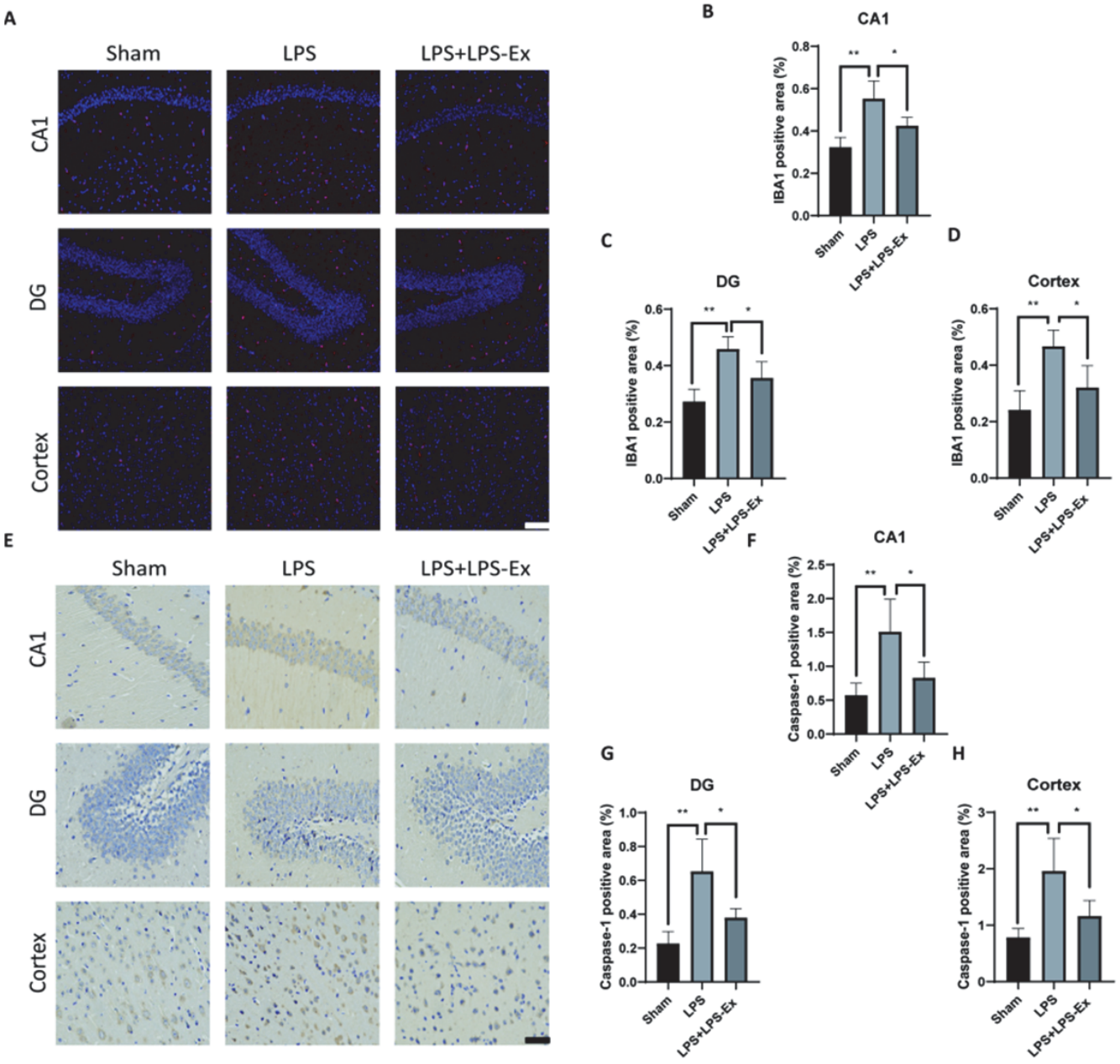

Fig. 5. LPS-Ex alleviates microglial activation, pyroptosis and neuronal apoptosis. (**A–D**) Changes of microglia in the cortex and hippocampus observed through fluorescence microscopy. (**E–H**) The distribution of caspase-1, the key protein of pyroptosis, in the cortex and hippocampus detected by immunohistochemistry; n = 6 per group. * P < 0.05, ** P < 0.01, *** P < 0.001. Scale bar = 50 μm. Data are presented as the mean ± SD. (*continued on the other side*)

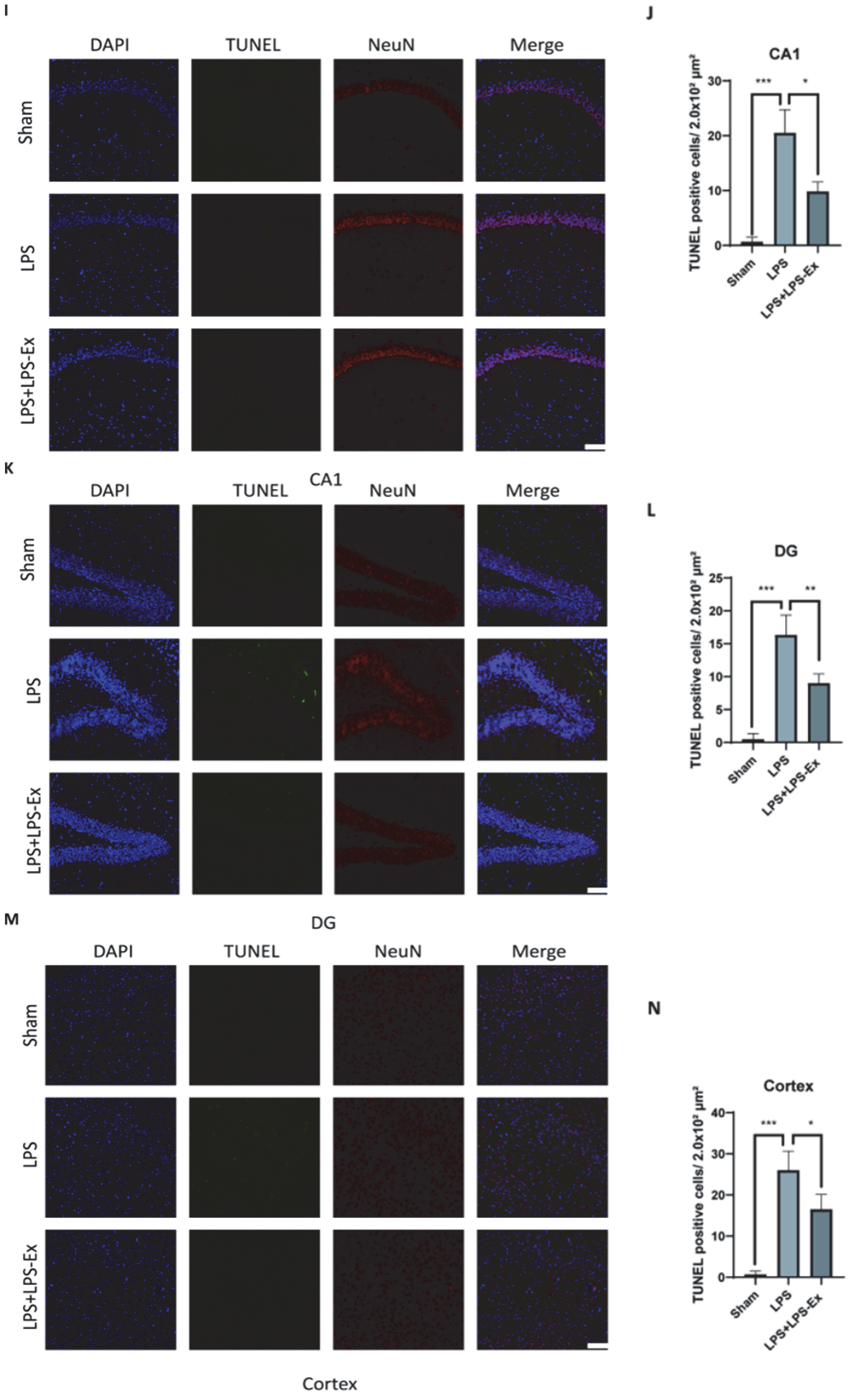

Fig. 5 (*continue*)**.** (**I–N**) Reduction in neuronal apoptosis in different regions of the brain detected through immunofluorescence and TUNEL staining, the TUNEL parts show apoptosis, the NeuN parts show neuron cells; n = 6 per group. * $P < 0.05$, ** $P < 0.01$, *** $P < 0.001$. Scale bar = 50 μm. Data are presented as the mean ± SD.

Discussion

This study confirmed through in vivo experiments that exosomes secreted by LPS-stimulated macrophages alleviate the neuroinflammatory response caused by systemic LPS-stimulated stimulation by reducing pyroptosis. From the research, we can draw three core conclusions. (1) LPS-Ex can reduce the levels of inflammatory factors. (2) LPS-Ex improves the neurological prognosis of mice by down-regulating the pyroptosis pathway and the NF-κB inflammatory pathway. (3) LPS-Ex reduces microglial activation and neuronal apoptosis.

Exosomes contain many biologically active molecules such as proteins, RNA, DNA, lipids and microRNAs (miRs) (Valadi et al., 2007). These bioactive molecules mediate exogenous intercellular communication, possibly targeting specific cell types, thereby altering their target cell function by providing proteins, lipids, and nucleic acids (Choi et al., 2015). Our experimental results confirmed that we successfully extracted exosomes and used them in subsequent experiments. Previous studies have shown that LPS-Ex exerts a protective effect on cerebral ischemia by transforming the functional polarization of microglia from M1 type to anti-inflammatory M2 type phenotype (Zheng et al., 2019). Our research has confirmed that LPS-Ex also has a neuroprotective effect in central nervous system inflammation.

Pyroptosis is a recently discovered inflammasome-mediated and caspase-1 dependent programmed cell death that is stimulated by a range of microbial or non-infectious stimuli (He et al., 2015). In addition, previous studies have shown that pyroptosis is usually associated with released cytoplasmic LDH (DiPeso et al., 2017). NF-κB is one of the most well-known inflammation-related transcription factors produced by almost all eukaryotic cells, regulating a large number of genes and signaling pathways involved in inflammation (Ma and Hottiger, 2016). García et al. (2015) and Liu et al. (2017) reported that melatonin inhibits the activation of NF-κB/NLRP3 by modulating the nuclear receptor. Another group demonstrated that NF-κB increases GSDMD transcription by binding to two proximal binding sites upstream of the gene promoter region. Our experimental results do indeed confirm that the pyroptosis pathway and the NF-κB signaling pathway are involved in central nervous system inflammation.

Therefore, the pyroptosis pathway and the NF-κB pathway are closely linked. Reports indicate that embryonic stem cell-derived exosomes inhibit doxorubicin-induced TLR4-NLRP3-mediated pyroptosis (Tavakoli Dargani and Singla, 2019). Therefore, it is feasible to regulate the mechanism of pyroptosis by the exosomal pathway. We found that LPS-Ex inhibited the pyroptosis pathway and the NF-κB pathway, improving neurological prognosis. Specifically, we first found that the expressions of caspase-1, NLRP3, ASC, and GSDMD decreased after 24 hours as detected by Western blotting. This result is consistent with the previous understanding of the mechanism by which exosomes regulate pyroptosis (Xiong et al., 2022). Meanwhile, we found that the expression of phosphorylated NF-κB and IκBα as well as the level of TLR4 decreased after exosome intervention. This is also in line with previous research reports on the NF-κB signaling pathway (Sun et al., 2020). Secondly, HE staining was performed to detect the histomorphological changes of neurons in the hippocampus and cortex. We found that LPS-Ex treatment could improve the changes in histological morphology. This is in line with previous studies on exosomes (Ni et al., 2019). Finally, the neurological deficits and cerebral edema of the mice were detected within 24 hours. We reached the conclusion that LPS-Ex can improve the prognosis of neurological function. This is consistent with the relevant research on the protection of neural function in mice by exosomes (Ni et al., 2019). Therefore, our results indicate that LPS-Ex treatment effectively attenuates LPS-induced neuroinflammation. The mechanism of LPS-Ex in central nervous system inflammation may be involved in the regulation of pyroptosis.

Microglia are macrophages that reside in the brain and respond quickly to nervous system inflammatory activation (Sun et al., 2020). Previous studies have found that pyroptosis can occur in neurons, astrocytes, and microglia in damaged brain tissue, thereby accelerating the induction of inflammation and neuronal death, and aggravating neurological functional outcomes (Zhang et al., 2024). Apoptosis is also widely present in damaged brain tissue (He et al., 2023). Our subsequent research confirmed that LPS-Ex alleviates microglial activation and neuronal apoptosis. First, we conducted a study on microglia in the cortex and hippocampus and found that the number of cells in different brain regions decreased after LPS-Ex treatment. This experimental result is consistent with previous studies on the regulatory role of exosomes in microglia (Ni et al., 2019). Then, we found that the distribution of caspase-1, a key protein for pyroptosis in the brain, decreased. This experimental result is consistent with previous research reports on caspase-1 (Sun et al., 2020).

Finally, we detected a reduction in neuronal apoptosis in different brain regions through TUNEL staining. Previous studies have reported that exosomes secreted by adipose-derived mesenchymal stem cells pretreated with hypoxia reduce neuronal apoptosis in rats with spinal cord injury (Liang et al., 2022). Our experimental results confirm that LPS-Ex treatment can also alleviate neuronal apoptosis in CNS inflammation.

Lipopolysaccharide-treated mice represent one of the more widely used models of neuroinflammation (Catorce and Gevorkian, 2016). In this study, we selected LPS-stimulated macrophage-derived exosomes because they can exhibit more anti-inflammatory effects than macrophage-derived exosomes (Zheng et al., 2019). Severe neuroinflammatory reactions can affect neurogenesis and aggravate neurological deficits by releasing inflammatory factors (Wang et al., 2018). Our results demonstrate that LPS-Ex has a certain anti-inflammatory effect, reduces the release of pro-inflammatory factors, and increases the production of anti-inflammatory factors.

Conclusion

Our results indicate that LPS-Ex relieves neuroinflammation by inhibiting the pyroptosis and NF-κB pathways. It can be used as a novel therapeutic strategy for neuroprotection and functional recovery in the onset of central nervous system inflammation.

Acknowledgements
Zhezhe Sun provided financial support for the research to be conducted and the preparation of the article. Zhezhe Sun participated in the research design and data collection, while Tao Ying was involved in the analysis and interpretation as well as the report writing.

Funding
The study was supported by Ningbo Health Technology Project, No: 2020Y12 and 2022Y12.

Ethical aspects and conflict of interest

The authors have no conflict of interest to declare.

References

Catorce MN, Gevorkian G (2016). LPS-induced Murine Neuroinflammation Model: Main Features and Suitability for Pre-clinical Assessment of Nutraceuticals. Curr Neuropharmacol 14(2): 155–164. DOI: 10.2174/1570159x14666151204122017.

Choi DS, Kim DK, Kim YK, Gho YS (2015). Proteomics of extracellular vesicles: Exosomes and ectosomes. Mass Spectrom Rev 34(4): 474–490. DOI: 10.1002/mas.21420.

Courtois G, Gilmore TD (2006). Mutations in the NF-kappaB signaling pathway: implications for human disease. Oncogene 25(51): 6831–6843. DOI: 10.1038/sj.onc.1209939.

Denzer K, Kleijmeer MJ, Heijnen HF, Stoorvogel W, Geuze HJ (2000). Exosome: from internal vesicle of the multivesicular body to intercellular signaling device. J Cell Sci 19: 3365–3374. DOI: 10.1242/jcs.113.19.3365.

DiPeso L, Ji DX, Vance RE, Price JV (2017). Cell death and cell lysis are separable events during pyroptosis. Cell Death Discov 3: 17070. DOI: 10.1038/cddiscovery.2017.70.

García JA, Volt H, Venegas C, Doerrier C, Escames G, López LC, Acuña-Castroviejo D (2015). Disruption of the NF-kappaB/NLRP3 connection by melatonin requires retinoid-related orphan receptor-alpha and blocks the septic response in mice. FASEB J 29(9): 3863–3875. DOI: 10.1096/fj.15-273656.

He C, Xu Y, Sun J, Li L, Zhang JH, Wang Y (2023). Autophagy and Apoptosis in Acute Brain Injuries: From Mechanism to Treatment. Antioxid Redox Signal 38(1–3): 234–257. DOI: 10.1089/ars.2021.0094.

He WT, Wan H, Hu L, Chen P, Wang X, Huang Z, et al. (2015). Gasdermin D is an executor of pyroptosis and required for interleukin-1beta secretion. Cell Res 25(12): 1285–1298. DOI: 10.1038/cr.2015.139.

Hsu SD, Lin FM, Wu WY, Liang C, Huang WC, Chan WL, et al. (2011). miRTarBase: a database curates experimentally validated microRNA-target interactions. Nucleic Acids Res 39(Database issue): D163–169. DOI: 10.1093/nar/gkq1107.

Hu X, Leak RK, Shi Y, Suenaga J, Gao Y, Zheng P, Chen J (2015). Microglial and macrophage polarization – new prospects for brain repair. Nat Rev Neurol 11(1): 56–64. DOI: 10.1038/nrneurol.2014.207.

Ishrat T, Mohamed IN, Pillai B, Soliman S, Fouda AY, Ergul A, et al. (2015). Thioredoxin-interacting protein: a novel target for neuroprotection in experimental thromboembolic stroke in mice. Mol Neurobiol 51(2): 766–778. DOI: 10.1007/s12035-014-8766-x.

Kayagaki N, Stowe IB, Lee BL, O'Rourke K, Anderson K, Warming S, et al. (2015). Caspase-11 cleaves gasdermin D for non-canonical inflammasome signalling. Nature 526(7575): 666–671. DOI: 10.1038/nature15541.

Lee MS, Hwang SK, Kim YE, Suh JK, Kim H, Lee SM, et al. (2019). Central nervous system vasculitis from Epstein-Barr virus-associated T/natural killer-cell lymphoproliferative disorder in children: A case report. Brain Dev 41(9): 820–825. DOI: 10.1016/j.braindev.2019.05.009.

Lee SW, Gajavelli S, Spurlock MS, Andreoni C, de Rivero Vaccari JP, Bullock MR, et al. (2018). Microglial Inflammasome Activation in Penetrating Ballistic-Like Brain Injury. J Neurotrauma 35(14): 1681–1693. DOI: 10.1089/neu.2017.5530.

Liu Z, Gan L, Xu Y, Luo D, Ren Q, Wu S, Sun C (2017). Melatonin alleviates inflammasome-induced pyroptosis through inhibiting NF-kappaB/GSDMD signal in mice adipose tissue. J Pineal Res 63(1). DOI: 10.1111/jpi.12414.

Ma B, Hottiger MO (2016). Crosstalk between Wnt/beta-Catenin and NF-kappaB Signaling Pathway during Inflammation. Front Immunol 7: 378. DOI: 10.3389/fimmu.2016.00378.

Man SM, Karki R, Kanneganti TD (2017). Molecular mechanisms and functions of pyroptosis, inflammatory caspases and inflammasomes in infectious diseases. Immunol Rev 277(1): 61–75. DOI: 10.1111/imr.12534.

Ni H, Yang S, Siaw-Debrah F, Hu J, Wu K, He Z, et al. (2019). Exosomes Derived From Bone Mesenchymal Stem Cells Ameliorate Early Inflammatory Responses Following Traumatic Brain Injury. Front Neurosci 13: 14. DOI: 10.3389/fnins.2019.00014.

Shi J, Gao W, Shao F (2017). Pyroptosis: Gasdermin-Mediated Programmed Necrotic Cell Death. Trends Biochem Sci 42(4): 245–254. DOI: 10.1016/j.tibs.2016.10.004.

Sun Z, Nyanzu M, Yang S, Zhu X, Wang K, Ru J, et al. (2020). VX765 Attenuates Pyroptosis and HMGB1/TLR4/NF-κB Pathways to Improve Functional Outcomes in TBI Mice. Oxid Med Cell Longev 2020: 7879629. DOI: 10.1155/2020/7879629.

Tavakoli Dargani Z, Singla DK (2019). Embryonic stem cell-derived exosomes inhibit doxorubicin-induced TLR4-NLRP3-mediated cell death-pyroptosis. Am J Physiol Heart Circ Physiol 317(2): H460–H471. DOI: 10.1152/ajpheart.00056.2019.

Valadi H, Ekström K, Bossios A, Sjöstrand M, Lee JJ, Lötvall JO (2007). Exosome-mediated transfer of mRNAs and microRNAs is a novel mechanism of genetic exchange between cells. Nat Cell Biol 9(6): 654–659. DOI: 10.1038/ncb1596.

Vezzani A, Granata T (2005). Brain inflammation in epilepsy: experimental and clinical evidence. Epilepsia 46(11): 1724–1743. DOI: 10.1111/j.1528-1167.2005.00298.x.

Wang Y, Huang Y, Xu Y, Ruan W, Wang H, Zhang Y, et al. (2018). A Dual AMPK/Nrf2 Activator Reduces Brain Inflammation After Stroke by Enhancing Microglia M2 Polarization. Antioxid Redox Signal 28(2): 141–163. DOI: 10.1089/ars.2017.7003.

Zhang X, Huang X, Hang D, Jin J, Li S, Zhu Y, Liu H (2024). Targeting pyroptosis with nanoparticles to alleviate neuroinflammatory for preventing secondary damage following traumatic brain injury. Sci Adv 10(2): eadj4260. DOI: 10.1126/sciadv.adj4260.

Zheng Y, He E, Wang P, Shi Y, Zhao L, Liang J (2019). Exosomes from LPS-stimulated macrophages induce neuroprotection and functional improvement after ischemic stroke by modulating microglial polarization. Biomater Sci 7(5): 2037–2049. DOI: 10.1039/C8BM01449C.